Boson peaks of glassy mono- and polyalcohols studied by inelastic neutron scattering

2000 J. Phys.: Condens. Matter 12 5143

(http://iopscience.iop.org/0953-8984/12/24/306)

J. Phys.: Condens. Matter **12** (2000) 5143–5154. Printed in the UK PII: S0953-8984(00)12374-4

Boson peaks of glassy mono- and polyalcohols studied by inelastic neutron scattering

Osamu Yamamuro†‖, Kouji Harabe†, Takasuke Matsuo†, Kiyoshi Takeda‡, Itaru Tsukushi§¶ and Toshiji Kanaya§

† Department of Chemistry and Microcalorimetry Research Centre, Graduate School of Science, Osaka University, Toyonaka, Osaka 560-0043, Japan
‡ Department of Chemistry, Naruto University of Education, Naruto, Tokushima 772-8502, Japan
§ Institute for Chemical Research, Kyoto University, Uji, Kyoto 611-0011 Japan

E-mail: yamamuro@chem.sci.osaka-u.ac.jp

Received 6 March 2000

Abstract. We have measured the inelastic neutron scattering spectra of the glasses of six mono- and polyalcohols; 1-propanol, ethylene glycol, propylene glycol, 1,3-propanediol, glycerol and threitol. Broad excitation peaks with peak top energy of 3–5 meV appeared in all of the $S(2\theta, E)$ spectra. These peaks were identified as boson peaks characteristic of glassy materials from the temperature dependence of the peak intensity. We found a systematic relation among the boson peak energy, the boson peak intensity per molecule and the hydrogen-bond density estimated as the ratio of the number of hydroxyl groups to that of carbon atoms (N_{OH}/N_C); the peak energy decreases and the peak intensity increases as hydrogen-bond density decreases. The present result indicates that the origin of the boson peak in network glasses is related to the flexible part in the network structure (e.g., non-hydrogen-bonded alkyl-groups in alcohol glasses). We also measured partially deuterated propanol ($CD_3CD_2CD_2OH$ and $CH_3CH_2CH_2OD$) and glycerol ($CD_2(OH)CD(OH)CD_2OH$ and $CH_2(OD)CH(OD)CH_2OD$). Both energy and intensity of the boson peak were not affected much by the partial deuteration, indicating that the hydrogen-bonding and non-hydrogen-bonding (alkyl) parts contribute to the boson peak cooperatively. The present result was compared with the predictions from a simple model recently developed by Nakayama *et al*.

1. Introduction

For most amorphous solids, a broad excitation peak is observed at 2–5 meV in their Raman and neutron scattering spectra. Heat capacity and thermal conductivity anomalies are also observed in the temperature region 5–20 K where the corresponding energy levels start to be thermally populated. Such a low-energy excitation, which is usually called the 'boson peak' from the temperature dependence of its intensity, is one of the current topics in condensed matter physics [1]. A number of studies have been done on various types of amorphous materials e.g., covalent-bonding network glasses, polymer glasses and van der Waals glasses. The former two classes of glasses have a strong network or chain in their structure while the third one has no definite local structure. The most interesting character of the boson peak is the universality of its occurrence in the narrow energy range (2–5 meV) independently of the bonding energy and local structure. The boson peak may be associated with the disordered (but locally ordered)

‖ Author to whom any correspondence should be addressed.
¶ Present address: Department of Physics, Chiba Institute of Technology, Narashino, Chiba 275-0023, Japan.

0953-8984/00/245143+12$30.00

and strained structure of the amorphous solids, but its origin and microscopic mechanism have not been explained with sufficient generality.

We have studied the excess vibrational states in the hydrocarbon glasses with simple molecular structures by measuring the heat capacity and neutron scattering [2–7]. In terms of the intermolecular forces, the hydrocarbon glasses are close approximations to the van der Waals glass and thus are readily compared with theoretical and molecular dynamics studies. It is also advantageous that the molecular mass can be changed systematically in a homologous series of the hydrocarbons. The absolute density of vibrational states obtained by our INS and low-temperature heat capacity data [2–5] showed that the number of vibrational states associated with the low energy excitation is 1–2 per molecule. This value is much larger than that of SiO_2 glass (<0.1 per atom). We found an interesting relation between the boson peak energy (E_{bp}) and the molecular mass (M); E_{bp} is proportional to $M^{-1/2}$ for all of the hydrocarbons examined [4, 5]. From these results, we proposed that the boson peak of molecular glasses arises from the librational motion of the molecules which is localized on two to four molecules.

In this study, we measured inelastic neutron scattering (INS) of mono- and polyalcohol glasses. Alcohol glasses are intermediate between covalent-bonding network glasses and van der Waals glasses. With their hydroxyl groups (–OH), they form intermolecular hydrogen bonds producing a weaker version of covalent atomic connectivity, while alkyl groups ($–C_nH_{2n+1}$) of alcohol molecules are flexible side chains in the hydrogen-bonded network structure. These side chains are analogous to dangling bonds or some defect structure in covalent-bonding network glasses. One can vary the flexibility of the network by changing molecular structure. This increases the number of experimentally controllable parameters. A boson peak has already been found in the INS experiments of glassy methanol (doped with 10% of water) [8], ethanol (including orientational glass) [9] and glycerol [10, 11]. Raman scattering [12–14], spectral hole-burning [15] and fluorescence spectroscopy using doped dye molecules [16–18] have also been performed to investigate the properties of the boson peaks of some alcohol glasses. The main purpose of the present study was to obtain systematic data on the boson peak as functions of the numbers of carbon atoms and OH groups in an alcohol molecule and to find a general rule determining the boson peak energy and intensity of the glassy alcohols. We have also measured partially deuterated propanol and glycerol. Since the incoherent scattering from hydrogen atoms is dominant, one can separately see the density of vibrational states associated with hydrogen-bonding and non-hydrogen-bonding parts.

2. Experiment

2.1. Samples

The samples examined in this study were 1-propanol (PR, $CH_3CH_2CH_2OH$, $M = 60$, $T_g = 96$ K), ethylene glycol (EG, $CH_2(OH)CH_2OH$, $M = 62$, $T_g = 153$ K), propylene glycol (PG, $CH_3CH(OH)CH_2OH$, $M = 76$, $T_g = 164$ K) 1,3-propanediol (PD, $CH_2(OH)CH_2CH_2OH$, $M = 76$, $T_g = 145$ K), glycerol (GL, $CH_2(OH)CH(OH)CH_2OH$, $M = 92$, $T_g = 184$ K) and DL-threitol (TH, $CH_2(OH)CH(OH)CH(OH)CH_2OH$, $M = 122$, $T_g = 229$ K), where the items in the brackets are the abbreviation symbol for the substance, chemical formula, molar mass and glass transition temperature, respectively. PR is a monoalcohol with only one OH group at the end of the carbon chain, EG, GL and TH are polyalcohols with one OH group on each carbon atom and PG and PD are polyalcohols with an OH group on two of three carbon atoms. PR, EG, PG and PD (all special grade) were purchased from Wako Pure Chemical Ind., Ltd. They were dried with sodium metal and purified by fractional distillation with a concentric-type rectifier. Glycerol (purity: >99.5%)

and DL-threitol (>97%) were purchased from Aldrich Chemical Co., Ltd., and used without purification. For ethylene glycol, about 10% of glycerol was doped to suppress the crystallization. This was found necessary in the previous heat capacity measurement [19]. The effect of the added glycerol was not important for the discussion in this paper. The partially deuterated alcohols PR-d_1 ($CH_3CH_2CH_2OD$, special grade) were purchased from Tokyo Kasei Kogyo, PR-d_7 ($CD_3CD_2CD_2OH$, 99.3%), PR-d_8 ($CD_3CD_2CD_2OD$, 99.3%), GL-d_3 ($CH_2(OD)CH(OD)CH_2OD$, 98.7%) and GL-d_5 ($CD_2(OH)CD(OH)CD_2OH$, 99.5%) were from CDN Isotope. The numbers after the chemical formula in the above descriptions are the percentage of deuteration.

2.2. Neutron scattering measurement

INS experiments on PR, EG, GL, TH, PR-d_1, PR-d_7, PR-d_8, GL-d_3 and GL-d_5 were performed on a direct geometry chopper-type TOF spectrometer AGNES (C3-1-1) [20] of the Institute of Solid State Physics, The University of Tokyo. It is installed at the steady cold neutron source of JRR-3M in Tokai, Japan. The wavelength of the incident neutron (selected by PG(002) monochrometer) was 4.22 Å (4.59 meV). The energy resolution of the elastic peak was 0.1 meV and the energy window was $\leqslant$20 meV. In the experiments for the normal samples, 61 ^{3}He tube counters were installed at 2θ = 20–34, 45–60, 70–84, and 95–109° with steps of 1°. This counter arrangement covers the scattering vector Q region of 0.5–2.4 $Å^{-1}$ for elastic scattering. For the partially and fully deuterated samples, the counters were installed only at a high angle region (2θ = 70–130°, with the step of 1°) to obtain high intensity. The corresponding Q region was 1.7–2.6 $Å^{-1}$ for elastic scattering.

The liquid samples were confined in the concentric double-cylinder aluminum can (35 mm in height, 14.5 mm in outer diameter, 14.0 mm in inner diameter of the outer cylinder) using an indium gasket. The outer diameter of the inner cylinder was varied to adjust the sample thickness. For the protonated samples, the sample thickness was 1 mm. The transmission of the neutron beam was calculated to be about 60% for all of the samples. The duration of the measurement was 15–20 h for each sample. For the deuterated samples, the thickness of the sample was selected in the range 0.5–2 mm to adjust the transmission of neutron beam to about 75–80%. The duration of the measurement was 20–30 h. Thus, we used rather a large quantity of the sample to obtain good counting statistics while compromising the accuracy since our main purpose was the comparison among several alcohol samples. All of the measurement was performed at 100 K, which is close to the glass transition temperature of PR and lower than those of other samples. PR was measured also at 70 K to check the absence of a quasielastic scattering due to relaxational effects at 100 K.

The raw scattering data, neutron counts (I) against time-of-flight (t_f), were processed into the dynamic structure factor $S(2\theta, E)$ by correcting for the effects of the background, counter efficiency, Jacobian $\mathrm{d}t_f/\mathrm{d}E$ etc following the established routine. We did not correct for the multiple scattering but confirmed that the shape of spectra was not distorted as described latter. The observed $S(2\theta, E)$ was determined almost exclusively by incoherent scattering from hydrogen atoms.

PR, GL, PG and PD were measured with the inverted geometry time-of-flight (TOF) spectrometer LAM-40 [21] installed at the pulsed spallation cold neutron source in the National Laboratory for High Energy Physics (KEK) in Tsukuba, Japan. PR and GL were measured both with AGNES and LAM-40 to examine the dependence of the INS spectrum on the instruments and sample thickness. In the LAM spectrometer, pulsed cold neutrons with a wide energy distribution are incident on the sample, and the scattered neutrons with fixed energy (4.59 meV) are selected by a PG(002) crystal analyser mirror and a Be filter, and detected by

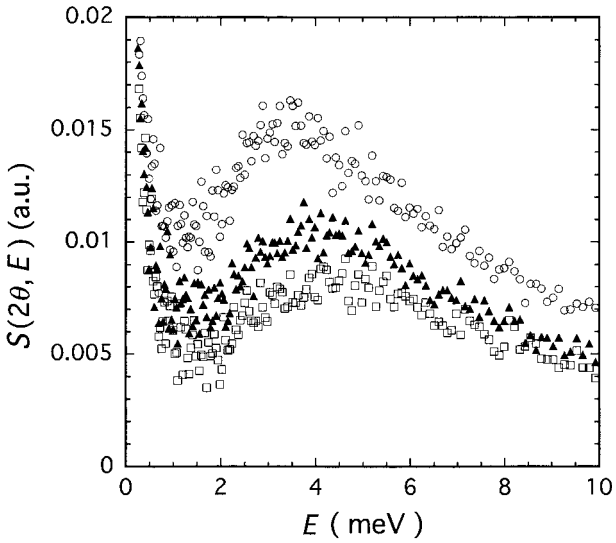

Figure 1. Dynamic structure factor $S(2\theta, E)$ of the glassy ethylene glycol (○), glycerol (▲) and threitol (□) observed by AGNES at 100 K. All of the data with different scattering angles were summed up to improve counting statistics; the mean Q value for the elastic peak was 1.5 Å^{-1}. The data were normalized by the integrated intensity of each sample.

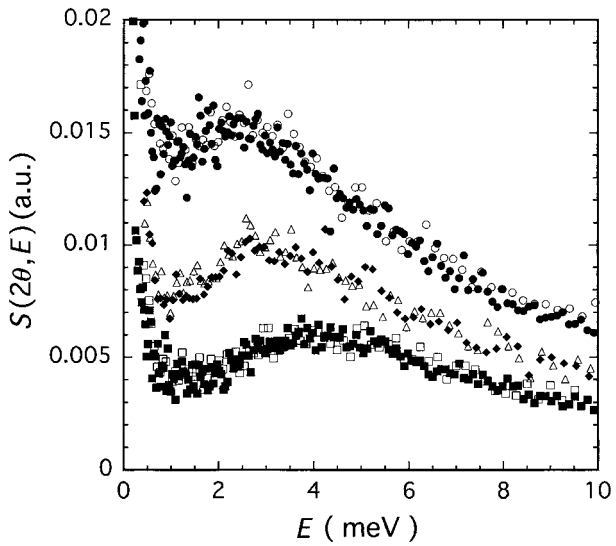

Figure 2. Dynamic structure factor $S(2\theta, E)$ of glassy propanol (○), propylene glycol (△), 1,3-propanediol (◆), and glycerol (□) observed by LAM-40 at 100 K. The data of propanol (●) and glycerol (■) by AGNES were also plotted for comparison of two spectrometers AGNES and LAM-40. All of the data with different scattering angles were summed up; the mean Q value for the elastic peak was 1.5 Å^{-1}. The data were normalized by the integrated intensity of each sample.

^{3}He counters at seven scattering angles 2θ. In this experiment, the scattering angles 2θ were set to 16, 32, 48, 64, 80, 96 and 112°. The energy resolution was 0.2 meV and the energy window extended to 10 meV. The magnitude of the scattering vector Q at the elastic position ranged from 0.4 to 2.5 Å^{-1}.

The sample liquids for the LAM experiments were also confined in the concentric double-cylinder aluminum can (115 mm in height, 14.0 mm in inner diameter of the outer cylinder, 13.6 mm in outer diameter of the inner cylinder, 0.20 mm in thickness of sample) using an indium gasket. The transmission of neutrons was calculated to be about 90%, which is much larger than the experiments on AGNES. The measurement was carried out at 100 K for all the samples. PG was measured at 100 and 160 K to examine the temperature dependence of the spectra. The duration of the experimental time was about 12 h for a given temperature. The observed TOF spectrum was converted to $S(2\theta, E)$ after making corrections for empty cryostat scattering, counter efficiency and the incident neutron spectrum.

3. Results and discussion

3.1. Boson peak

Figure 1 shows the $S(2\theta, E)$ of glassy EG, GL and TH observed by AGNES at 100 K, and figure 2 the $S(2\theta, E)$ of glassy PR, PG, PD and GL by LAM-40 at 100 K. The data of PR and GL, plotted in figure 2, were collected both by AGNES and LAM-40. All of the data with different scattering angles were summed up to improve counting statistics. The mean Q value was 1.5 Å^{-1} for both AGNES and LAM-40 at the elastic position. The data were normalized by the integrated intensity of each sample, which is roughly proportional to the number of hydrogen atoms irradiated by neutron beam. The data by LAM-40 were scaled against the AGNES data. EG, GL and TH in figure 1 are polyalcohols with one OH group at each carbon atom; their carbon numbers $N_C (= N_{OH})$ are 2, 3, and 4, respectively. On the other hand, PR, PG, PD, and GL in figure 2 have the same N_C (= 3) but different numbers N_{OH} of OH groups (PR: 1, PG: 2, PD: 2, GL: 3); PG has two OH groups at the centre and end carbons while PD at both end carbons. Hence, figures 1 and 2 demonstrate the effect of N_C (or molecular mass) and N_{OH} on the boson peak, respectively.

A boson peak was clearly observed in all of the spectra. The boson peak energy and intensity depended on N_C and N_{OH}. Further discussion is left for the following sections. The data by LAM-40 and AGNES agreed remarkably well. This indicates that both instruments are reliable and that multiple scattering, which was significant for AGNES data, did not deform the shape of spectra. This is consistent with the fact that the intensity of the boson peak is much smaller than that of the elastic peak (less than 1%) and so the elastic–inelastic and inelastic–elastic processes dominate the multiple scattering. Agreement with the previous data by Wuttke *et al* [10, 11] on GL is also to be noted.

Figure 3 shows the $S(2\theta, E)$ of PG at 100 K (same as in figure 2) and 160 K. The data at 160 K were scaled by the Bose factor to 100 K. They agreed with each other giving further evidence for the boson characteristics of the peaks. Similar tests for Bose scaling were done also for PR (at 70 K) and EG (at 150 K) on AGNES. These results also indicate that no relaxational phenomenon appeared at 100 K for all of the examined alcohols. This is quite natural because their glass transition temperatures are larger than 100 K ($T_g \approx 100$ K only for PR).

3.2. Density of vibrational states

For the comparison of the boson peak intensities of the alcohols examined, we calculated the density of vibrational states $G(E)$ by assuming the one phonon scattering process [22]. $G(E)$ was calculated for each of seven counters (for LAM-40) or seven groups of counters (for AGNES) with different E–Q relations and then summed over counters. The correction for the Debye–Waller factor and the extrapolation to $Q = 0$ were not performed. The summed

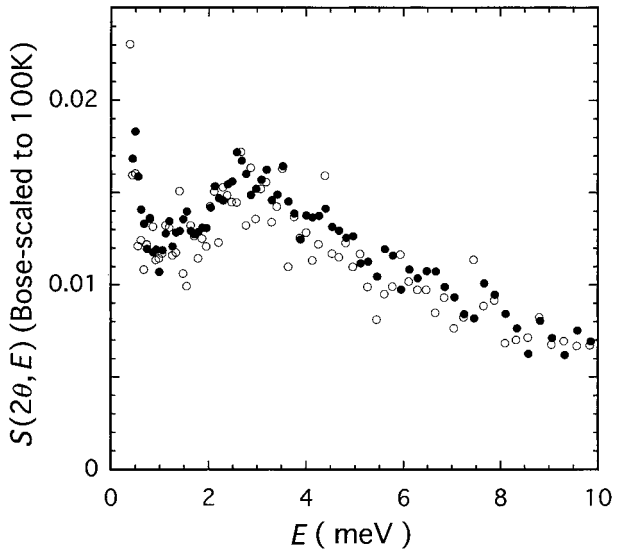

Figure 3. Dynamic structure factor $S(2\theta, E)$ of propylene glycol observed by LAM-40 at 100 K (●) and 160 K (○). The data at 160 K were scaled by the Bose factor to the data at 100 K.

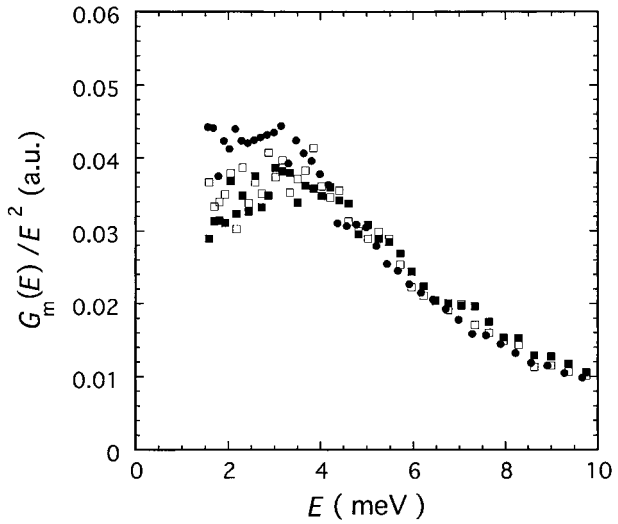

Figure 4. Density of vibrational states per molecule divided by energy squared $G_m(E)/E^2$. ●: ethylene glycol, □: glycerol, ■: threitol. Comparison among the alcohols with different carbon numbers; each carbon atom has one OH group.

$G(E)$ data were reduced to the values per molecule $G_m(E)$ by using the molar volume and the number of hydrogen atoms in a molecule for each substance. Figures 4 and 5 give the molar density of vibrational states divided by energy squared $G_m(E)/E^2$; this plotting style facilitates comparison with the Debye model (where $G_m(E)/E^2$ is constant) and also magnifies the boson peak region. Figures 4 and 5 correspond to figures 1 and 2, respectively (the data by AGNES have been omitted from figure 5). One sees in figure 4 that $G(E)/E^2$ of EG, GL and TH are similar to each other with respect to the energy and intensity. In figure 5, however,

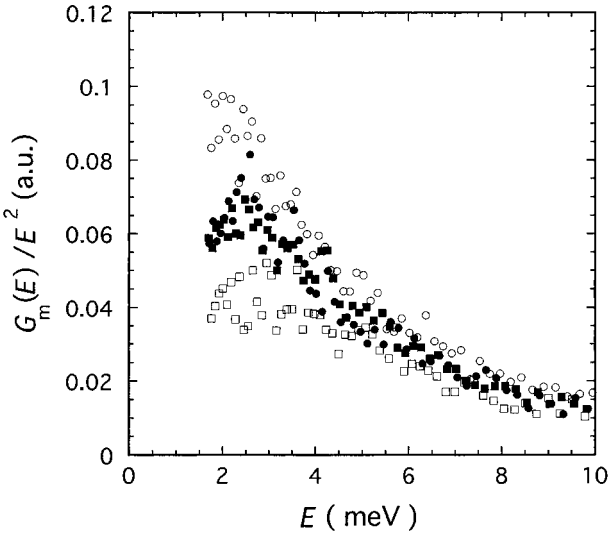

Figure 5. Density of vibrational states per molecule divided by energy squared $G_m(E)/E^2$. ○: propanol, ●: propylene glycol, ■: 1,3-propanediol, □: glycerol. Comparison among the alcohols with the same carbon number (= 3) and different OH group numbers.

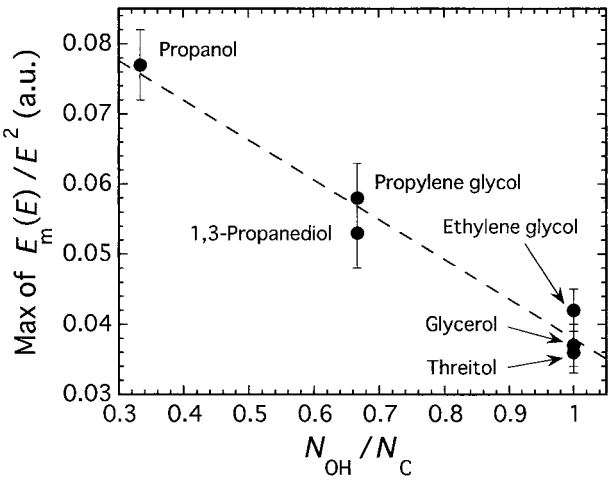

Figure 6. Maximum of the molar density of vibrational states divided by energy squared. The data were plotted as a function of the hydrogen-bond density N_{OH}/N_C (see text for the details).

$G(E)/E^2$ of PR, PG (or PD) and GL are clearly different from each other. $G(E)/E^2$ of PG is similar to that of PD. Thus $G(E)/E^2$ does not depend on N_C but on N_{OH}. It is noteworthy that the intensity difference was observed in the LAM-40 data (figure 5) where the multiple scattering was negligible in the present context so that their intensity is more reliable than that of AGNES.

To investigate the effect of N_{OH} for all of the alcohol glasses, we introduce a new parameter 'hydrogen-bond density' defined as the ratio of the number of hydroxyl groups to that of carbon atoms (N_{OH}/N_C). The hydrogen-bond density is 1 for EG, GL and TH, 2/3 for PG and PD and 1/3 for PR. As the hydrogen-bond density increases, the flexible part of a glass

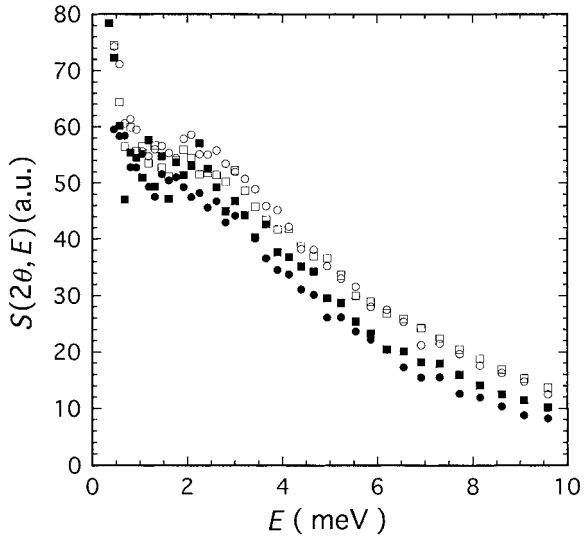

Figure 7. Dynamic structure factor $S(2\theta, E)$ of partially-deuterated propanol glasses observed by AGNES at 100 K. □: propanol-d_1 ($CH_3CH_2CH_2OD$), ●: propanol-d_7 ($CD_3CD_2CD_2OH$). The data of fully protonated (○) and deuterated samples (■) are also plotted for comparison. All of the data from different counters were summed up and normalized by dividing the integrated intensity for each samples. The mean Q value for the elastic scattering was 2.0 $Å^{-1}$.

(alkyl groups) decreases and the hydrogen-bond network becomes more rigid. We plotted the maximum values of $G_m(E)/E^2$ as a function of the hydrogen-bond density in figure 6. The maximum value was determined by averaging several points around the peak top. The uncertainty was about ±0.003 for the AGNES data and ±0.005 for the LAM data. Figure 6 shows that $G_m(E)/E^2$ decreases as the hydrogen-bond density increases for the alcohols with N_C of 2, 3 and 4. This tendency is mainly due to the change in boson peak intensity rather than the Debye part since the Debye levels of the plotted substances are expected to be similar because they have similar molecular structures and mass densities; the sound velocities of these substances have not been measured. We conclude that the boson peak intensity increases as the hydrogen-bond density decreases and the flexible part of the glass increases.

3.3. Effect of partial deuteration

Figures 7 and 8 show the $S(2\theta, E)$ of glasses of partially deuterated propanol and glycerol, respectively. The data of fully protonated samples are also plotted for comparison. All of the data from different counters were summed up and normalized by dividing by the integrated intensity for each sample. The mean Q value for elastic scattering was 2.0 $Å^{-1}$. Since the incoherent scattering from hydrogen atoms is dominant, one can separately see the density of vibrational states associated with hydrogen-bonding parts (e.g., –OH of $CD_3CD_2CD_2OH$) and non-hydrogen-bonding parts (e.g., $CH_3CH_2CH_2$– of $CH_3CH_2CH_2OD$) in the data of partially deuterated samples.

For both propanol and glycerol, the $S(2\theta, E)$ curves of the partially deuterated samples are similar in shape though they are slightly different in intensity probably because of the multiple scattering effects. The effect of coherent scattering, which is comparable with incoherent scattering only for PR-d_7 ($\sigma_{inc}/\sigma_{coh} = 1.5$), did not deform the shape of the spectra in any significant way as revealed by the data of fully deuterated propanol

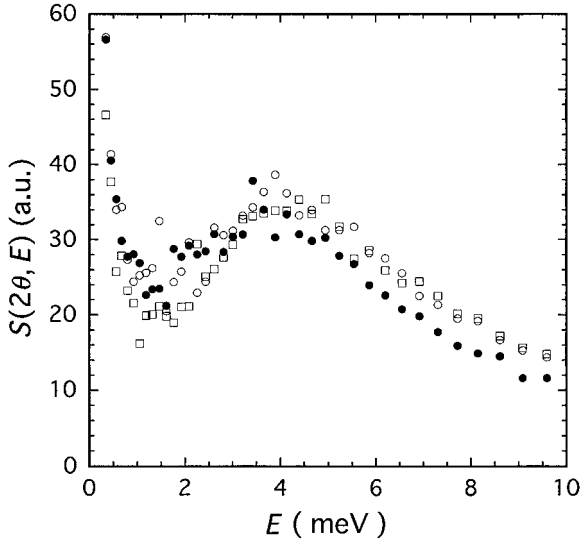

Figure 8. Dynamic structure factor $S(2\theta, E)$ of partially deuterated glycerol glasses observed by AGNES at 180 K. □: glycerol-d_3 (CH_2(OD)CH(OD)CH_2OD), ●: glycerol-d_5 (CD_2(OH)CD(OH)CD_2OH). The data of fully protonated samples (○) are also plotted for comparison. All of the data from different counters were summed up and normalized by dividing the integrated intensity for each samples. The mean Q value for the elastic scattering was 2.0 $Å^{-1}$.

(coherent scatterer) in figure 7. Wuttke *et al* [10, 11] have obtained similar results for GL-d_3 (CH_2(OD)CH(OD)CH_2OD). The present result indicates that the hydrogen-bonding and non-hydrogen-bonding (alkyl) parts contribute to the boson peak cooperatively. Hence the boson peak arises from the vibration localized in a region larger than one alcohol molecule. From the result on the density of states (the peak intensity decreases as the hydrogen-bond density increases), one may visualize the simplest molecular model of the boson peak as the intramolecular vibration of alkyl group. However this is clearly wrong as revealed in figures 7 and 8. Cooperative motions of the main and side chains have been observed also in the neutron scattering study of partially deuterated polymers [23].

3.4. Molecular mass dependence of the boson peak energy

The boson peak energies in $S(2\theta, E)$ spectra are plotted in figure 9 as functions of inverse square root of molecular mass. The literature data for the hydrocarbon glasses [2–7], methanol (MT, CH_3OH, $M = 32$, $T_g = 103$ K) with 10% of added water [8], ethanol (ET, CH_3CH_2OH, $M = 46$, $T_g = 90$ K) [9] and glycerol [10, 11] are also plotted for comparison. The uncertainty of E_{bp} was roughly estimated to be $\pm 10\%$ of E_{bp} though this estimation is difficult because the data were obtained by various neutron scattering spectrometers and various researches. For the hydrocarbon glasses, the data lie on a straight line passing through zero implying the simple mass dependence of a harmonic oscillator with the same force constant [4, 5]. The same mass dependence has been pointed out also in a spectral hole-burning study [15]. However, the alcohol glasses have a quite different mass dependence from that of the hydrocarbon glasses; E_{bp} decreases with increasing $M^{-1/2}$ for polyalcohols (EG, GL, TH) and is almost constant for monoalcohols (MT, ET, PR). For PG and PD, the boson peak energy is intermediate between these two. It can be concluded that the boson peak energy of alcohol glasses does not depend on the molecular mass in a simple way.

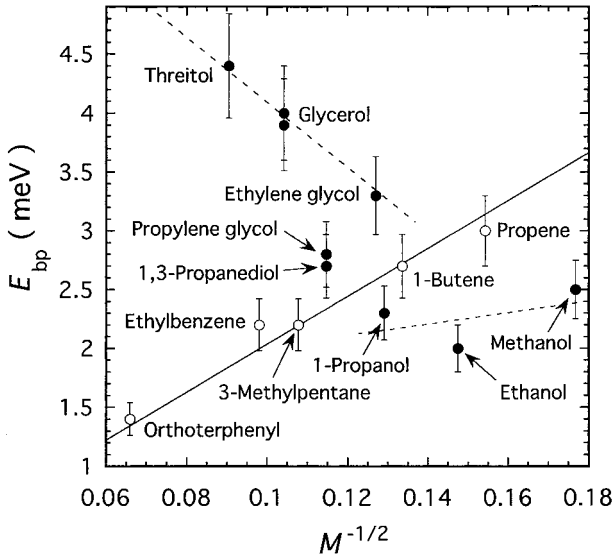

Figure 9. Peak top energies of the boson peak of $S(2\theta, E)$ plotted as functions of inverse square root of molecular mass. The literature data for the hydrocarbon glasses [2-7], methanol [8], ethanol [9] and glycerol [10, 11] are also plotted for comparison. Open and closed circles represent the data of hydrocarbon and alcohol glasses, respectively.

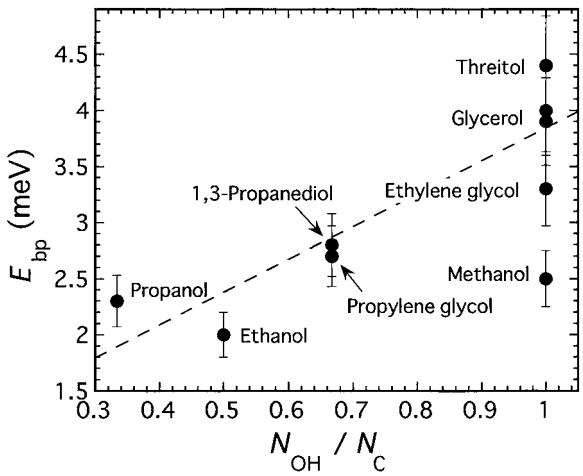

Figure 10. Peak top energies of the boson peak of $S(2\theta, E)$ plotted as functions of the hydrogen-bond density N_{OH}/N_C. The literature data for methanol [8], ethanol [9] and glycerol [10, 11] are also plotted.

We have found another systematic relation for the boson peak energy of alcohol glasses. As shown in figure 10, E_{bp} increases as the hydrogen-bond density increases for the alcohols with N_C of 3 (GL, PG, PD, PR) and those with N_C of 2 (EG, ET). MT ($N_C = 1$) is exceptional in this respect, which is acceptable because it is a very small molecule and so the molecular overall libration is more important to the boson peak than in the larger alcohol molecules. The hydrogen-bond density is thus an important parameter determining not only the boson peak intensity but also the peak energy.

3.5. Origin of the boson peak in glassy alcohols

The results obtained in the present study for alcohol glasses are summarized as follows. (1) The hydrogen-bonding and non-hydrogen-bonding (alkyl) parts contribute to the boson peak cooperatively. (2) The boson peak energy increases as the hydrogen-bond density increases. (3) The boson peak intensity decreases as the hydrogen-bond density increases. There are various models for the boson peak but they are phenomenological or not applicable to the alcohol glasses with both natures of network and van der Waals glasses [1]. Recently, a simple microscopic model applicable to the alcohol glasses was proposed by Nakayama *et al* [24–26]. As the first attempt to explain the present results, we compare the present results with the predictions by the Nakayama model.

The Nakayama model has been conceived to describe the dynamics of network glasses. It assumes a pair of regular main chains and side components randomly attached to the main chain. The side components represent defects, local distortion, or any additional weakly bonded parts in the glass. The number of the units forming the main chains is larger than that of the side components. The force constant between the adjacent main-chain units is larger than that between the main chain unit and the side component attached to it. The latter force constant is assumed to be distributed over a certain range of values to represent the structural disorder. Lattice dynamics calculation showed the occurrence of a strongly localized vibration at low energies and an intermediately localized vibration with higher excitation energy. The former vibration, which corresponds to the boson peak, is the collective anti-phase vibration of the main chain and side component. This model agrees with the experimental results of SiO_2 glass [27, 28] and water [29, 30], especially for the Q dependence of the excitation energy.

If the hydrogen-bond network of alcohol glasses is identified with the main chains and the non-hydrogen-bonding part (alkyl group) with the side component, the present experimental results are consistent with the predictions by the Nakayama model. First, the coherent vibration suggested by the result (1) of the above summary corresponds nicely to the strongly localized vibration in the model (the collective anti-phase vibration of a group of the main chain and the side component). Secondly, if the force constant between the main chain and the side component becomes smaller, which is equivalent to increasing the mass of the side component, the peak energy becomes smaller in agreement with our result (2). Finally, if the number of side components becomes larger, the peak intensity of course becomes larger as our result (3).

Thus, the Nakayama model explains the present experimental results qualitatively. We think that the model describes correctly the origin of the boson peak of the network glasses, even though the correspondence with the real microscopic structure of the glass is not very clear because of the simplifications made in the modelling. We hope that the model will be developed into a more quantitative form which can predict the boson peak energy and intensity quantitatively. It is also desirable to create a new model applicable to the boson peaks of any amorphous materials ranging from covalent-bonding network glasses to van der Waals glasses.

Acknowledgment

The authors thank Professor Tsuyoshi Kajitani (Tohoku University), Professor Shin-ichi Shamoto (Tohoku University) and Dr Yasuhiro Ono (Tohoku University) for their help in the experiments on the AGNES spectrometer, and Dr Kaoru Shibata (Tohoku University) for the experiments on the LAM-40 spectrometer. The authors are grateful to Professor Tsuneyoshi Nakayama (Hokkaido University) for the discussion on his model. This work is financially supported by the Ministry of Education, Science and Culture, Japan Grant-in-Aid for Scientific Research on Priority Areas No 07236230 and Grant-in-Aid for Scientific Research No 08640486 and 09304066.

References

[1] For example: Phillips W A 1987 *Rep. Prog. Phys.* **50** 1657
Buchenau U 1989 *Dynamics of Disordered Materials* ed D Richter, A J Dianoux, W Petry and J Teixeira (Berlin: Springer)
Buchenau U 1993 *Phase Transitions and Relaxation in Systems with Competing Energy Scales* ed T Riste and D Sherrington (Dordrecht: Kluwer)
Frick B and Richter D 1995 *Science* **267** 1939
[2] Yamamuro O, Matsuo T, Takeda K, Kanaya T, Kawaguchi T and Kaji K 1996 *J. Chem. Phys.* **105** 732
[3] Yamamuro O, Tsukushi I, Matsuo T, Takeda K, Kanaya T and Kaji K 1997 *J. Chem. Phys.* **106** 2997
[4] Lindqvist A, Yamamuro O, Tsukushi I and Matsuo T 1997 *J. Chem. Phys.* **107** 5103
[5] Yamamuro O, Tsukushi I, Matsuo T, Takeda K, Kanaya T and Kaji K 1997 *Prog. Theor. Phys. Suppl.* **126** 89
[6] Yamamuro O, Tsukushi I, Kanaya T and Matsuo T 1999 *J. Phys. Chem. Solids* **60** 1537
[7] Tsukushi I, Yamamuro O, Yamamoto K, Takeda K, Kanaya T and Matsuo T 1999 *J. Phys. Chem. Solids* **60** 1541
[8] Bermejo F J, Alonso J, Criado A, Mompeán F J, Martínez J L, García-Hernández M and Chahid A 1992 *Phys. Rev.* B **46** 6173
[9] Ramos M A, Vieira S, Bermejo F J, Dawidowski J, Fischer H E, Schober H, González M A, Loong C K and Price D L 1997 *Phys. Rev. Lett.* **78** 82
[10] Wuttke J, Hernandez J, Li G, Coddens G, Cummins H Z, Fujara F, Petry W and Sillescu H 1994 *Phys. Rev. Lett.* **72** 3052
[11] Wuttke J, Petry W, Coddens G and Fujara F 1995 *Phys. Rev.* E **52** 4026
[12] Kojima S 1993 *Phys. Rev.* B **47** 2924
[13] Yoshihara A, Sato H and Kojima S 1997 *Prog. Theor. Phys. Suppl.* **126** 423
[14] Kojima S, Yamaura T and Takagi Y 1997 *Prog. Theor. Phys. Suppl.* **126** 427
[15] Renge I 1998 *Phys. Rev.* B **58** 14 117
[16] Ichino Y, Kanematsu Y, Hashimoto N and Kushida T 1996 *J. Lumin.* **66/67** 358
[17] Kanematsu Y, Ichino Y, Hashimoto N and Kushida T 1998 *J. Lumin.* **76/77** 632
[18] Kanematsu Y 1998 *Optical Properties of Low-dimensional Materials* vol 2 (Singapore: World Scientific) ch 2
[19] Takeda K, Yamamuro O, Tsukushi I, Matsuo T and Suga H 1999 *J. Mol. Struct.* **479** 227
[20] Kajitani T, Shibata K, Ikeda S, Kohgi M, Yoshizawa H, Nemoto K and Suzuki K 1995 *Physica* B **213/214** 872
[21] Inoue K, Ishikawa Y, Watanabe N, Kaji K, Kiyanagi Y, Iwasa H and Kohgi M 1984 *Nucl. Instrum. Methods* A **238** 401
[22] Marshall W and Lovesey S W 1971 *Theory of Thermal Neutron Scattering* (Oxford: Clarendon)
[23] Kanaya T, Kawaguchi T and Kaji K 1996 *J. Chem. Phys.* **104** 3841
[24] Nakayama T and Sato N 1998 *J. Phys.: Condens. Matter* **10** L41
[25] Nakayama T 1998 *Phys. Rev. Lett.* **80** 1244
[26] Nakayama T 1999 *Physica* B **263/264** 243
[27] Benassi P, Krisch M, Masciovecchio C, Mazzacurati V, Monaco G, Ruocco G, Sette F and Verbeni R 1996 *Phys. Rev. Lett.* **77** 3835
[28] Arai M, Inamura Y, Otomo T, Kitamura N, Bennington S M and Hannon A C 1999 *Physica* B **263/264** 268
[29] Sette F, Ruocco G, Krisch M, Bergmann U, Masciovecchio C, Mazzacurati V, Signorelli G and Verbeni R 1995 *Phys. Rev. Lett.* **75** 850
[30] Ruocco G, Sette F, Bergmann U, Krisch M, Masciovecchio C, Mazzacurati V, Signorelli G and Verbeni R 1995 *Nature* **379** 521